A Source of Response Regulator Autophosphatase Activity: The Critical Role of a Residue Adjacent to the SpoOF Autophosphorylation Active Site †

ARTICLE *in* BIOCHEMISTRY · JUNE 1998

Impact Factor: 3.02 · DOI: 10.1021/bi9729615 · Source: PubMed

6 AUTHORS, INCLUDING:

James Zapf
Visionary Pharmaceuticals Inc
30 PUBLICATIONS **888** CITATIONS
SEE PROFILE

Kottayil I Varughese
University of Arkansas for Medical Sciences
111 PUBLICATIONS **2,512** CITATIONS
SEE PROFILE

A Source of Response Regulator Autophosphatase Activity: The Critical Role of a Residue Adjacent to the Spo0F Autophosphorylation Active Site†

James Zapf, Madhusudan, Charles E. Grimshaw, James A. Hoch, Kottayil I. Varughese,* and John M. Whiteley

Department of Molecular and Experimental Medicine, NX-1, The Scripps Research Institute, 10550 North Torrey Pines Road, La Jolla, California 92037

Received December 2, 1997; Revised Manuscript Received March 31, 1998

ABSTRACT: Two-component signaling systems are used by bacteria, plants, and lower eukaryotes to adapt to environmental changes. The first component, a protein kinase, responds to a signal by phosphorylating the second component; a response regulator protein that often acts by inducing the expression of specific genes. Response regulators also have an autophosphatase activity that ensures that the proteins are not permanently activated by phosphorylation. The magnitude of this activity varies by at least 1000-fold between various response regulators, and the molecular features responsible for this varied autophosphatase activity have not been clearly defined. Using wild-type and mutant derivatives of the sporulation response regulator Spo0F, it has been demonstrated that a key residue in determining the magnitude of this activity is that at position 56 of Spo0F∼P; this residue is adjacent to the site of phosphorylation, Asp 54. For example, Spo0F∼P K56N has a 23-fold greater autophosphatase activity ($t_{1/2}$ = 8 min) than wild-type Spo0F∼P ($t_{1/2}$ = 180 min). It is suggested that, by analogy to the GTPase activity of $p21^{ras}$ and by examining the crystallographic structure of Spo0F, that the carboxyamide of the mutant Asn 56 may favorably position a catalytic water near the protein acyl phosphate to promote Spo0F∼P K56N hydrolysis. It is also deduced that Lys 56 in the wild-type protein is critical for the efficient interaction and phosphoryl transfer between Spo0F and it's cognate protein kinase, KinA. Comparison of the known response regulators shows that inefficient autophosphatases ($t_{1/2}$ on the order of hours) typically contain an amino acid residue with a long side chain at the position equivalent to 56 in Spo0F, whereas efficient autophosphatases ($t_{1/2}$ on the order of minutes) frequently contain a residue with a carboxyamide or carboxylate side chain at this position. It appears that, by altering residues adjacent to the active site, the autophosphatase activity of response regulator proteins has been attenuated to match the diverse biological roles played by these proteins.

Bacteria, plants, and some lower eukaryotic organisms sense and adapt to environmental changes through the action of two-component signal transduction systems (*1*). These systems control the expression of virulence and drug resistance factors in several pathogenic organisms and are potential targets for antimicrobial therapeutic agents (*2*). "Two-component" systems typically consist of an autophosphorylating histidine protein kinase (*3*) and a response regulator protein, which is activated by phosphorylation at an aspartate residue (*4*). In response to unfavorable growth conditions, such as nutrient deprivation or high cell density, some bacteria will halt normal cell division and begin the developmental process of sporulation, leading to heat-resistant refractile spores. Sporulation in *Bacillus subtilis* is controlled by an expanded version of the two-component system termed the phosphorelay (*5, 6*). In the first step of this series of phosphorylation reactions, one or more protein histidine kinases (KinA, KinB, and KinC) bind ATP and autophosphorylate at a histidine residue. The phosphoryl moiety on these kinases is then transferred to Asp 54 of Spo0F, a response regulator. Spo0F∼P serves as a substrate for the third protein, Spo0B, which transfers the phosphate to Spo0A, a response regulator/transcription factor. This multiprotein phosphorelay controls the level of Spo0A∼P, the active form of Spo0A, which functions by stimulating the expression of genes required for sporulation. The flow of phosphate in the phosphorelay is controlled by a sophisticated regulatory mechanism which involves the action of phosphatases specific for Spo0F and Spo0A (*7*).

Response regulators are defined by a sequence of about 120 residues and five highly conserved residues form the phosphorylation active site. For Spo0F, they are Asp10, Asp 11, Asp 54, Thr 82, and Lys 104. Response regulators can occur as a portion of a multidomain protein (e.g., NarL and BvgS) or alone as a single domain protein (e.g., Spo0F and CheY). Despite the homology used to group these proteins in a single superfamily (*8*), response regulators have been found to have varied biochemical properties. In particular, the hydrolysis rate of phosphorylated response regulators

† This investigation was supported in part by Grants GM54246 (K.I.V.), GM19416 (J.A.H.), and GM45727 (J.M.W.) from the National Institute of General Medical Sciences (USGMS) and the National Institutes of Health and by the Sam and Rose Stein Charitable Trust. The Scripps Research Institute Mass Spectroscopy facility is supported by the Lucille P. Markey Charitable Trust and NIH Grant GM 44154. This is publication number 11272-MEM from The Scripps Research Institute.

* Corresponding author. Phone: 619-784-7945. Fax: 619-784-7966. E-mail: kiv@scripps.edu.

S0006-2960(97)02961-9 CCC: $15.00
Published on Web 05/08/1998

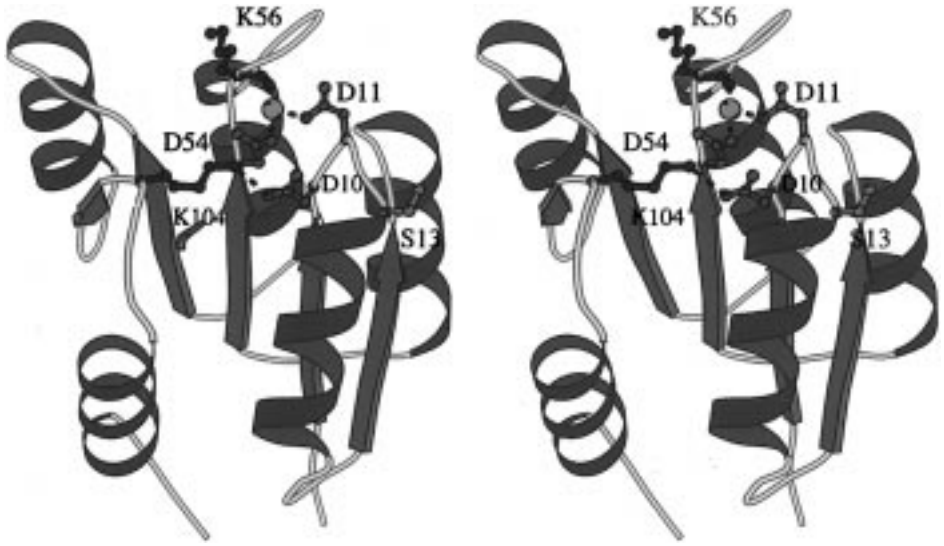

FIGURE 1: A stereoview of the structure of the Ca^{2+}-bound Spo0F Y13S active site. Ribbon diagram showing helices in purple, β strands in green and β turns and loops in yellow. The highly conserved residues in the aspartate pocket, Asp 10, Asp 11, Asp 54, and Lys 104 along with residue 13 are shown in ball-and-stick format. The side chain of Lys 56, also shown in ball-and-stick format, lies near the active site at the top of the figure. The Ca^{2+} ion present in the structure is shown as an orange sphere, however, both Mg^{2+} and Ca^{2+} ions bind to Spo0F and both ions catalyze phosphoryltransfer from KinA∼P to Spo0F. Hydrogen bonds and calcium coordination are shown as black dots.

Table 1: Autodephosphorylation Half-Life Values for Various Response Regulators in the Presence of a Divalent Cation

response regulator	residue 56[a]	$t_{1/2}$ (min)	ref
CheY	Asn	0.5	*11*
CheB	Glu	∼0.02	*38*
NtrC	Val	4.0	*43*
Spo0F K56N	Asn	8.0	this work
NarL	Asn	30	*44*
PhoB	Met	81[b]	*45*
OmpR	Met	∼120	*29*
Spo0F	Lys	180	this work
VanR	Met	540	*46*

[a] Residue at the position equivalent to 56 of Spo0F. [b] A value of 15 min is also reported for PhoB∼P (*47*).

differ by approximately 3 orders of magnitude, with Spo0F∼P being one of the most "stable" phosphorylated response regulators (Table 1). Response regulators are only active when phosphorylated, and their acyl phosphate hydrolysis is thought to be catalyzed by an autophosphatase activity (*9*), which controls the amount of time these proteins remain in an activated state. The magnitude of the autophosphatase activity seems to be appropriately matched to the biological roles of the regulators. For example, the chemotaxis response regulator, CheY∼P, autodephosphorylates in a matter of seconds (*10*), about the same amount of time bacteria take to change the direction of swimming. In contrast, sporulation in *B. subtilis* is initiated over at least an hour, and Spo0F autodephosphorylates over the course of several hours. The conserved Lys and Thr residues probably function in the autophosphatase activity of phosphorylated response regulators since mutating either of these active-site residues in CheY∼P (Thr 87 and Lys 109) (*10, 11*) decreases this activity about 6-fold. However, the structural features that make some response regulators more efficient autophosphatases than others have not been clearly defined. In one of the few cases where structural comparisons can be made "stable", Spo0F (*12*) is superficially similar to two "unstable" response regulators CheY (*13*) and NarL (*14*) as rms deviations of their Cα atoms with Spo0F are only 2.8 and 1.8 Å, respectively. There are, however, significant differences between the structures in the environment adjacent to the phosphorylation active site. In particular, the Spo0F active site is protected by the side chain of Lys 56 (Figure 1), whereas the CheY and NarL active sites are more open because an Asn occupies this position. Moreover, a possible model for Spo0F∼P built using computer graphics shows that the side chain of Lys 56 could interact with the phosphoryl oxygens,[1] and it is hypothesized that this favorable interaction may contribute to the "stability" of Spo0F∼P.

This report describes experiments indicating that the magnitude of the autophosphatase activity of Spo0F∼P and the efficient phosphoryl transfer between Spo0F and KinA∼P depend on the type of residue at position 56 and suggests how the properties of different amino acid residues at this position might influence autophosphatase activity at the molecular level.

MATERIALS AND METHODS

Mutagenesis and Protein Purification. Mutations in *spo*0F were constructed by oligonucleotide directed site-specific mutagenesis using the method of Kunkel (*15*). All mutations were confirmed by DNA sequencing of the final plasmid. Expression in *Escherichia coli* and purification were performed as previously described for Spo0F (*16*), Spo0A (*17*), Spo0B, and KinA (*6*). The molecular weights of Spo0F proteins were verified by MALDI mass spectroscopy.

Phosphorylation Kinetics. Protein phosphorylation reactions containing 50 mM EPPS,[2] pH 8.5, 50 mM KCl, 20 mM $MgCl_2$, 5% glycerol (phosphorylation buffer), 0.5 mM [γ-^{32}P]ATP (∼2000 cpm/pmol), 0.5 μM KinA and 10 μM

[1] K. I. Varughese, unpublished observation.

[2] Abbreviations: EPPS, *N*-(2-hydroxyethyl)piperazine-*N*′-(3-propanesulfonic acid); PP, disodium pyrophosphate; potassium phosphate K_3PO_4.

Spo0F were incubated at 25 °C and quenched at various times between 15 s and 2 h by transferring 20 μL aliquots into 5 μL of SDS sample buffer. Samples were analyzed by SDS−PAGE on 15% gels followed by phosphorimaging (Molecular Dynamics) as previously described (*16*). Phosphorelay reactions contained 0.5 μM Spo0B and 10 μM Spo0A in addition to the components listed above. Protein phosphorylation was also measured using a filter binding assay procedure similar to that described by Ninfa et al. (*3*). Identical results were obtained with both SDS−PAGE and filter binding assays. For filter binding assays, aliquots (8 μL) were spotted onto glass fiber filters (Whatman GF/A) and immediately washed on a vacuum manifold three times with 10% TCA (w/v) containing 1% (w/v) disodium pyrophosphate (PP). Filters were stored at −80 °C to await further processing. Once all aliquots were taken, filters were placed in a plastic basket and immersed in ice-cold 10% TCA/1% PP. By stirring the solution with a magnetic stir bar, filters were washed once (30 min) in ice-cold 10% TCA/1% PP, twice (30 min) in ice-cold 5% TCA/1% PP, and once (5 min) in ice-cold 70% ethanol. After drying, radioactivity was quantitated by phosphorimaging. The specific activity of [γ-^{32}P]ATP was determined from serial dilution of ATP stock solutions spotted onto glass fiber filters. The purity of [γ-^{32}P]ATP was determined by thin-layer chromatography on PEI cellulose using 2 M $LiCl_2$ as solvent. Kinetic simulations and fitting were performed using numerical integration with the DOS versions of the programs Kinsim v. 3.3 and Fitsim v. 1.6 (*18*).

Fluorescence Quenching. Quenching experiments were performed with 2 μM of Spo0F mutants Y13W or Y13W + K56N in 50 mM HEPES, pH 7.0, and 250 mM KCl employing 1.0 M $MgCl_2$ or 3.0 M KCl as ligand. Titrations were carried out as described (*19*). Apparent Mg^{2+} dissociation constants were obtained by nonlinear least-squares fitting of the fluorescence quenching data to the equation below (*20*):

$$F_0/F = 1 + M[\mathrm{L}]/([\mathrm{L}] + K_\mathrm{d}) + N[\mathrm{L}] \qquad (1)$$

where F and F_0 are the fluorescence intensities in the presence and absence of ligand, respectively; [L] is the free ligand concentration; M the ratio of F_0/F at saturating ligand concentrations; and N a term that was included to account for possible dynamic or collisional quenching. Data are presented as F_0/F versus $MgCl_2$ concentration to show that saturation was achieved during the titration.

Inorganic Phosphate Release. Spo0F protein (25 μM) was incubated at 25 °C with KinA (5 μM) in phosphorylation buffer in the presence of 0.5 mM [γ-^{32}P]ATP (200 cpm/pmol). Control reactions containing KinA, Spo0F protein, or no protein showed that none of the proteins had a measurable ATPase activity when incubated alone. Samples were quenched at times from 2 min to 5 h by mixing 2 μL aliquots of the reaction mixture with 8 μL of 70 mM EDTA, pH 8.0, and freezing the diluted aliquots in a dry ice ethanol bath. Samples (1 μL) were analyzed by PEI cellulose TLC. Phosphorimager units were converted to phosphate concentration using a standard curve made from serially diluted [γ-^{32}P]ATP.

Spo0F∼P Isolation and Autodephosphorylation. Spo0F phosphorylation reactions (0.5 mL) were carried out as described above by incubating for 30 min at 25 °C. Reactions were applied to 1.0 mL of damp hydroxyapatite (Bio-Gel HTP from Bio-Rad) contained in a centrifugal column preequilibrated in phosphorylation buffer at 25 °C. Samples were absorbed to the resin for 1 min then eluted by centrifuging (30 s) in a picofuge (Stratagene). Solutions containing various concentrations of potassium phosphate (K_3PO_4) were prepared by diluting a 1 M stock of K_3PO_4, pH ∼9.0, into phosphorylation buffer. The resin was washed two times with 300 μL of 15 mM K_3PO_4, two times with 300 μL of 50 mM K_3PO_4, and two times with 300 μL of 200 mM K_3PO_4. At each step, the column was placed onto a 1.5 mL eppendorf tube containing 100 μL of a 50% slurry of Chelex 100 in water. The eluant was collected by centrifuging the column for 30 s in a picofuge. The addition of Chelex 100 followed by freezing in a dry ice ethanol bath was found to prevent hydrolysis of the phosphoproteins. The bulk of Spo0F∼P eluted in the second 50 mM K_3PO_4 wash; whereas, KinA∼P, ATP, and Pi eluted in the 200 mM K_3PO_4 washes. Spo0F∼P protein was now centrifuged for 2 min at 4 °C to pellet the Chelex 100 resin, and the supernatant containing Spo0F∼P was extracted and diluted 2-fold into phosphorylation buffer containing either 70 mM $MgCl_2$ or 40 mM EDTA. To carry out autophosphatase activity assays, samples were incubated at 25 °C and aliquots (8 μL) were quenched at various times by spotting onto a glass fiber filter, which were processed as described above.

Other Methods. Molar absorption values for Spo0F and its mutants were derived from amino acid analyses used to initially quantitate the protein. Spo0F proteins containing Tyr at position 13 exhibited a molar absorption of 7114 M^{-1} cm^{-1}, and Spo0F proteins containing Trp at position 13 exhibited a molar absorption of 8837 M^{-1} cm^{-1}. The concentration of KinA, Spo0B, and Spo0A solutions were estimated by the Bradford dye binding assay using BSA as a standard (*21*).

RESULTS

Phosphorylation and Magnesium Affinity of Spo0F Proteins. The mutant proteins (K56M, K56A, K56N, Y13W, and the double mutant Y13W + K56N) were overproduced and purified via chromatography on DEAE-Trisacryl and hydroxyapatite using similar procedures to those described for the wild-type protein (*6*, *16*), which suggested that the overall response regulator structural framework and chemistry was not changed by the mutations. Furthermore, all the proteins were phosphorylated by KinA and ATP (Figure 2, left panel) and could transfer phosphate to the next component in the phosphorelay, Spo0B, as can be seen by the production of Spo0A∼P, the terminal product of the sporulation phosphorelay (Figure 2, right panel). Although phosphorylated Spo0F and Spo0B are not apparent for the two Spo0F K56N lanes on the right of the autoradiogram, phosphor image analysis reveals low levels of phosphorylation for these mutants. Among the mutant Spo0F proteins, only K56M could be phosphorylated to the same extent as wild-type; however, all the mutant proteins reached a steady-state phosphorylation level at a slower rate than wild-type (Figure 3). Thus, the type of residue at position 56 of Spo0F affects the phosphorylation properties of this response regulator.

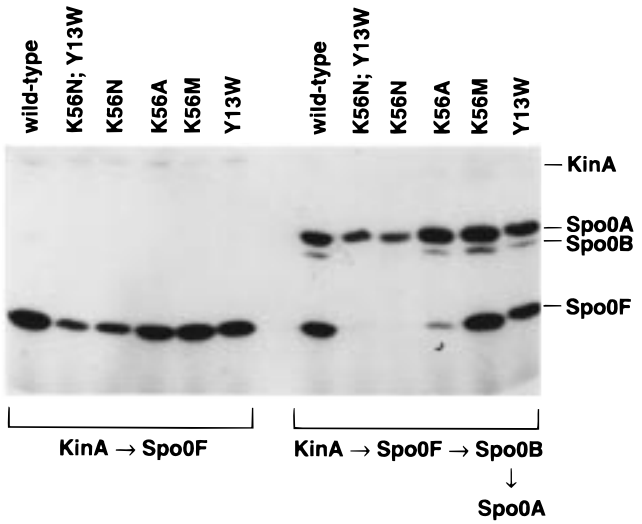

FIGURE 2: Autoradiogram after SDS−PAGE of the phosphorelay proteins. (Left) Phosphorylation of wild-type and mutant Spo0F proteins by KinA protein kinase. (Right) Participation of Spo0F proteins in the phosphorelay. The KinA and phosphorelay reactions were incubated 3 and 30 min, respectively, and were carried out as described in the Materials and Methods.

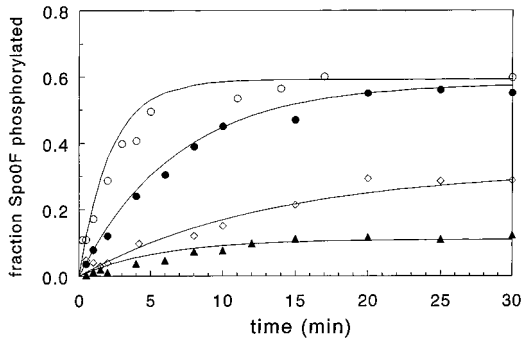

FIGURE 3: Time course of phosphotransfer from KinA and ATP to Spo0F proteins: wild-type Spo0F (○), K56M (●), K56A (◇), and K56N (▲). Phosphorylation reactions were carried out and analyzed by SDS−PAGE and a filter binding assay as described in the Materials and Methods. The lines drawn represent the results of simulations and fitting carried out as described in the Results.

To incorporate an active-site responsive fluorescent probe into Spo0F, the natural Tyr at position 13 was replaced with Trp (shown as a Ser in Figure 1). The Y13W mutation did not appear to alter the response regulator structure since the two Spo0F proteins containing this substitution (Spo0F Y13W and the double mutant Spo0F Y13W + K56N) were phosphorylated at the same rate and to the same extent as the corresponding Spo0F proteins containing Tyr at this position. Titration with Mg^{2+} induced similar fluorescence quenching profiles for both Y13W and Y13W + K56N proteins, yielding K_d values of 25 and 30 mM, respectively (Figure 4). A comparable value for the Mg^{2+} dissociation constant ($K_d = 20$ mM) has been determined independently for wild-type Spo0F using NMR (*22*). The similar Mg^{2+} binding affinity of Spo0F Y13W and Spo0F Y13W + K56N indicates that substitutions at position 56 essentially do not affect divalent cation binding.

Indirect Measurement of Spo0F∼P Hydrolysis by the Release of Inorganic Phosphate from ATP. If the type of residue at position 56 affects the autodephosphorylation rate of Spo0F∼P (k_3 in eq 2), some mutants should release inorganic phosphate from ATP at rates different from that

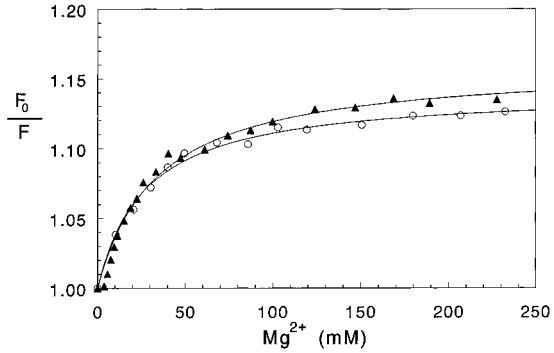

FIGURE 4: Quenching of Spo0F Y13W (○) and Y13W + K56N (▲) fluorescence by added $MgCl_2$. Quenching experiments were performed as described in the Materials and Methods. F_0 and F correspond to the protein fluorescence in the absence and presence of Mg^{2+}, respectively. The lines represent nonlinear least-squares fits to eq 1 yielding the following constants: for Spo0F Y13W, $K_d = 25$ mM, $M = 0.14$, $N \approx 0$; for Spo0F Y13W + K56N, $K_d = 30$ mM, $M = 0.16$, $N \approx 0$.

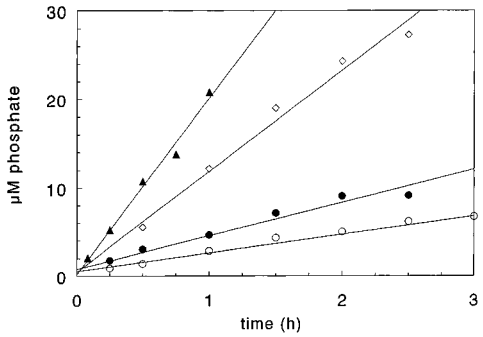

FIGURE 5: Release of ^{32}Pi from [γ-^{32}P]ATP by KinA and various Spo0F proteins: wild-type Spo0F (○), K56M (●), K56A (◇) and K56N (▲). Data were collected as described in the Materials and Methods. Rates of phosphate accumulation were determined from fitting data to a straight line.

seen for wild-type protein. This prediction is confirmed by the results shown in Figure 5, which record the rate of inorganic phosphate release from ATP measured in the presence of KinA and various Spo0F mutants. The least phosphorylated protein in Figure 2, Spo0F K56N, released phosphate the fastest ($k = 19.5$ μM/h) while the most highly phosphorylated protein [wild-type (K56)] released phosphate the slowest ($k = 2.0$ μM/h). The Spo0F proteins K56A and K56M released phosphate at rates between these two extremes with values of 11.5 μM/h and 5.0 μM/h, respectively. These data establish that an altered rate of phosphate hydrolysis occurs as a result of the K56 substitutions. Further, the rapid rate at which phosphate is produced indicates that the forward flow of phosphate, from ATP through KinA∼P and Spo0F∼P to inorganic phosphate, is still comparatively efficient with each mutant.

Autophosphatase Activity of Spo0F Proteins. Measuring the autodephosphorylation rate of Spo0F∼P proteins requires the separation of KinA and ATP from the response regulator. All the phosphorylated Spo0F proteins could be quickly and selectively eluted from a hydroxyapatite column, leaving KinA, nucleotides, and Pi bound to the matrix. The short time (∼2 min) required to carry out this procedure even allowed the isolation of Spo0F∼P K56N. The autodephosphorylation rates of phosphorylated Spo0F proteins in the presence of Mg^{2+} (Figure 6A) mirrored the extent to which these proteins were phosphorylated (Figure 3). Wild-type

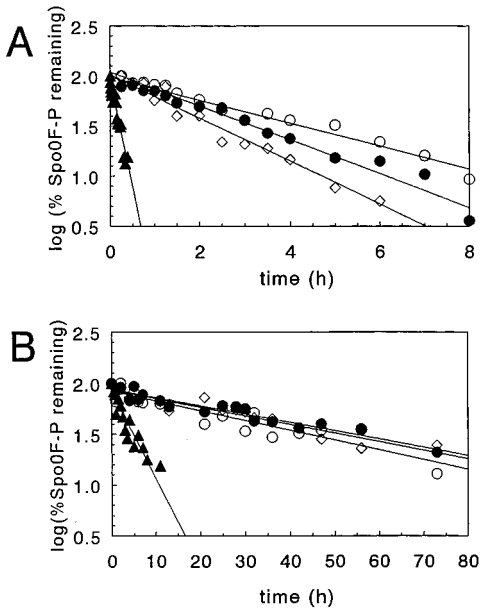

FIGURE 6: Autodephosphorylation of Spo0F∼P proteins: wild-type Spo0F (○), K56M (●), K56A (◇) and K56N (▲). Reactions were carried out at 25 °C and analyzed by a filter binding assay as described in the Materials and Methods. (A) Spo0F∼P proteins in the presence of $MgCl_2$. (B) Spo0F∼P proteins in the presence of 70 mM EDTA.

Table 2: Autophosphatase Activity Half-Life Values and Simulation Constants for Spo0F Proteins

	autophosphatase activity		simulation constants[a]	
Spo0F protein	$t_{1/2}$ (min) with Mg^{2+}	$t_{1/2}$ (min) without Mg^{2+}	k_2 (min^{-1})	k_{-2} (min^{-1})
wild-type	180 ± 30	1860 ± 360	0.250	0.170
K56M	132 ± 30	1980 ± 240	0.085	0.056
K56A	78 ± 20	1800 ± 300	0.025	0.041
K56N	8 ± 2	264 ± 30	0.021	0.074
Y13W	204 ± 45	1860 ± 300		
Y13W + K56N	6 ± 3	nd[b]		

[a] Derived from simulation and fitting of the data in Figure 3 to eq 2 where values of k_3 were entered as fixed constants. Values of K_3 were calculated from the half-life values shown for Spo0F∼P proteins in the presence of Mg^{2+} ion in the left-hand side of this table. Half-life values can be converted to rate constant values using the relationship $k = \ln 0.5/t_{1/2}$. [b] Not determined.

Spo0F had the longest phosphoprotein half-life (Table 2), the highest level of phosphorylation (59%) and the slowest rate of Pi release from ATP among the Spo0F proteins. In contrast, Spo0F K56N had the shortest phosphoprotein half-life, the lowest level of phosphorylation (11%), and fastest rate of Pi release from ATP. Spo0F K56M and Spo0F K56A have phosphoprotein half-lives similar to wild-type (Table 2). Among the fluorescent reporter mutants, Spo0F Y13W had a phosphoprotein half-life comparable to wild-type, and the double mutant Spo0F Y13W + K56N had a phosphoprotein half-life resembling Spo0F K56N (Table 2). These results further verify that the Y13W substitution did not perturb the response regulator structure. When the phosphorylated Spo0F proteins were treated with Chelex and EDTA to remove Mg^{2+}, phosphoprotein half-lives increased about an order of magnitude (Figure 6B and Table 2). Thus, the autodephosphorylation rate is reduced 10−30-fold by removing Mg^{2+}, verifying that Mg^{2+} also stimulates this activity (*23*). In the presence of SDS, the wild-type and mutant Spo0F∼P proteins all had nearly the same $t_{1/2}$ values (∼840 ± 120 min). Thus, denatured phosphoprotein hydrolyzed faster than nondenatured wild-type phosphoprotein in the absence of Mg^{2+}, suggesting that the natural conformation of Spo0F∼P can protect the acyl phosphate from hydrolysis. Overall, the greatest effect on formation and stability of the phosphorylated protein was caused by the K56N substitution, which caused an approximately 10-fold increase in the rate of phosphorylated response regulator hydrolysis in both the presence and absence of Mg^{2+}.

Simulation of the Phosphoryl-Transfer Reaction between KinA∼P and Spo0F Proteins. The slower rates by which Spo0F mutants reach a steady-state level suggest that the mutant proteins bind and/or accept phosphate from KinA∼P poorly compared to wild-type Spo0F (Figure 3). Thus, Lys 56 may play a role in both the phosphoryl transfer and autophosphatase activities of Spo0F, and both of these factors affect the extent of Spo0F phosphorylation reached at steady state. To estimate how the changing levels of autophosphatase activity affect the rate at which various Spo0F proteins are phosphorylated, kinetic simulations were performed according to the reaction sequence below:

$$\text{KinA} + \text{ATP} \overset{K_A}{\rightleftharpoons} \text{KinA}\sim\text{P} + \text{ADP}$$

$$\text{KinA}\sim\text{P} + \text{Spo0F} \underset{k_{-2}}{\overset{k_2}{\rightleftharpoons}} \text{Spo0F}\sim\text{P} + \text{KinA} \qquad (2)$$

$$\text{Spo0F}\sim\text{P} \xrightarrow{k_3} \text{Spo0F} + \text{Pi}$$

For these simulations, the concentration of KinA∼P was assumed to be maintained at a constant concentration by the autophosphorylation reaction since ATP was available in a large excess. This simplifying assumption is supported by SDS−PAGE and phosphorimager analysis that shows KinA∼P concentration is constant throughout the time course of the phosphotransfer reactions. Further, KinA does not act as a phosphatase of Spo0F∼P or stimulate the intrinsic autophosphatase activity of this phosphoprotein,[3] therefore the autodephosphorylation rate measured for each Spo0F∼P protein alone (Figure 6) was introduced as a fixed value of k_3 into each simulation. Finally, the forward and backward constants k_2 and k_{-2} thus depend both on binding of Spo0F to KinA∼P and catalysis of phosphoryl transfer, and these contributions cannot be separated using the present data. The results of the simulations are shown in Figure 3 as solid lines and closely predict the rate and extent of phosphoprotein formed with the various Spo0F proteins. From the derived constants k_2 and k_{-2} (Table 2), the interaction and phosphoryl transfer with KinA∼P is efficient with wild-type, intermediate with K56M, and poor with the K56A and K56N Spo0F proteins. The latter two seem to interact with equal efficiency.

DISCUSSION

Two-component signal transduction systems influence cell viability because they control chemotaxis, sporulation, osmotic, and other fundamental responses to changes in the cell environment (*24*). In response to positive stimuli, the

[3] Ling Wang and James A. Hoch, unpublished observation.

protein histidine kinase phosphorylates the response regulator, which then carries out some action, usually specific gene activation. Negative stimuli counteract the positive signals by a variety of mechanisms including activating phosphatase activities specific for response regulators (*25*, *26*). Thus, a regulatory network integrates several such physiological signals to control the outcome of many two-component signaling processes (*27*). Phosphorylation of the response regulator portion of the protein usually mediates signaling by activating a second catalytic domain (*17*, *28*). Some abbreviated response regulators, like Spo0F, lack such a second domain, and the consequences of phosphorylation must be conformational changes that alter the way Spo0F interacts with the additional proteins in the pathway, in this instance, Spo0B. The inherent autophosphatase activity of Spo0F modulates these forward effects and deactivates the response regulator. To understand the factors affecting the autophosphatase activity of a phosphorylated response regulator, the influence of residues in the vicinity of the active site, in particular the role of residue 56 of Spo0F∼P, has been examined by recording and comparing the kinetic properties of a series of mutant derivatives.

The structural comparison of Spo0F, CheY, and NarL response regulators suggested that residue 56 of Spo0F may affect the autophosphatase activity of Spo0F∼P. Because of the close proximity of the Lys 56 side chain to the phosphorylation active site in Spo0F structures, features such as the positive charge, length, and hydrophobicity of the Lys side chain may help protect the acyl phosphate of Spo0F∼P from hydrolysis and thus reduce the autophosphatase activity. To test these possibilities, a series of mutants at position 56 of Spo0F were constructed in order to probe the effects of charge (Lys to Met), length (Lys to Ala), and the combination of length and hydrogen bond potential (Lys to Asn) of this side chain on the autodephosphorylation rate of Spo0F∼P.

Properties of Spo0F Phosphoproteins. All the mutant proteins were phosphorylated by KinA∼P and could participate in the phosphorelay (Figure 2), but they were phosphorylated at a slower rate than wild-type (Figure 3). Mutant proteins having short side-chains (K56A and K56N) were phosphorylated to a lesser extent than proteins having long side chains (wild-type and K56M). This lower level of protein phosphorylation may arise from several factors, such as altered divalent cation binding, an increased rate of phosphoprotein hydrolysis, a decreased binding affinity for KinA∼P, a decreased rate of phosphoryl transfer from KinA∼P, or a composite of these. Divalent cation binding at the active site of response regulators is catalytically essential for both phosphorylation and for stimulating the autophosphatase activity of these proteins (*13*, *23*). The positive charge of the Lys 56 side chain could affect the binding of a divalent cation at the active site and thus influence the phosphorylation properties of Spo0F. However, quenching experiments with fluorescent versions of wild-type Spo0F (Y13W) and mutant Spo0F (Y13W + K56N) showed that Mg^{2+} affinity was not changed by the K56N substitution.

An increased Spo0F∼P hydrolysis rate, however, is substantiated by the increased rate of inorganic phosphate production from ATP seen with the mutant proteins (Figure 5). Indeed, the autodephosphorylation rates measured for various K56 mutants are 1.4−23 times faster than those for wild-type Spo0F (Figure 6 and Table 2), demonstrating that the type of residue at position 56 is a key factor governing the magnitude of this activity. The largest increase in the rate of Spo0F∼P hydrolysis resulted from the Lys to Asn change, which generated a mutant phosphoprotein that was ∼10-fold less stable than wild-type or the Spo0F∼P K56A mutant. Moreover, like the chemotaxis response regulator CheY∼P (*29*), the dephosphorylation rate of Spo0F∼P K56N could be decreased by 2 orders of magnitude when denatured with SDS, which implies that rapid autodephosphorylation of Spo0F∼P K56N results from the inherent catalytic activity of a conformationally intact response regulator.

Interaction and Phosphoryl Transfer between KinA∼P and Spo0F Proteins. In addition to affecting the autodephosphorylation rate, residue 56 of Spo0F also affects the interaction and phosphoryl transfer between this response regulator and KinA∼P. A poor interaction between Spo0F mutants and KinA∼P appears as a slow initial rate of mutant protein phosphorylation (Figure 3). For example, the Lys 56 to Ala mutation has been shown by Tzeng and Hoch (*30*) to cause a sporulation-defective phenotype. Furthermore, the mutant was found to increase the apparent Km of Spo0F for KinA∼P and also decrease the phosphoryl transfer rate between these two proteins. In support of these conclusions, kinetic simulations of the phosphorylation of the Spo0F proteins show that the low phosphorylation levels of mutant proteins studied here arise from slow phosphotransfer between KinA∼P and Spo0F mutants and to a lesser degree from the elevated autophosphatase activity of Spo0F mutants. The kinetic simulation and fitting (Figure 3) also yielded values for the constants (k_2 and k_{-2}) (Table 2) describing the binding and phosphotransfer between KinA∼P and Spo0F proteins. Comparison of the constants derived for the wild-type and mutant proteins suggests that the amine moiety as well as the length of the Lys 56 side chain are factors that allow this residue to promote the interaction between Spo0F and KinA∼P. Spo0F mutants lacking these elements of length and charge in the side chain at residue 56 (Spo0F K56A and K56N) still interact with KinA∼P but do it poorly. The lower phosphorylation level of Spo0F K56N relative to Spo0F K56A appears to be due mostly to the more rapid autodephosphorylation rate of the K56N relative to the K56A mutant as these proteins interact with KinA∼P with nearly equal efficiency. Thus, residue 56 plays dual roles by modulating the autophosphatase activity and also the interaction of Spo0F with it's cognate kinase KinA∼P.

Possible Catalytic Roles of Residue 56. The Lys 56 to Asn substitution appears to accelerate Spo0F∼P hydrolysis by a mechanism that does not exclusively depend on Mg^{2+} since Spo0F∼P K56N is ∼10-fold less stable than wild-type or K56A Spo0F∼P in both the presence or the absence of this divalent cation. Viewing Spo0F∼P hydrolysis as phosphoryl transfer from Spo0F∼P to water permits comparison of this reaction to what is generally known about phosphoryl-transfer reactions. In particular, divalent cations are thought to catalyze phosphoryl-transfer reactions by several means, including activating an attacking nucleophile, activating the protein acyl phosphate for attack by polarizing the P-0 or C-0 bonds, and neutralizing negative charge (*31*). Some of the same functions can be provided by a polar side chain just as well as by a metal ion (*13*). In such a

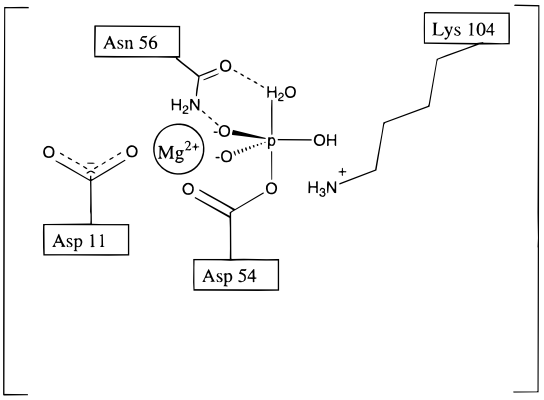

FIGURE 7: Transition state proposed for Spo0F∼P hydrolysis. A divalent cation such as Mg^{2+} may be coordinated in the active-site by Asp 11 and phosphate oxygen(s). Lys 104 is thought to be required for activation after phosphorylation. The side chain of Asn 56 is shown orienting a water molecule and interacting with the phosphointermediate.

mechanism, the Asn 56 side chain could work in parallel to a divalent cation to promote protein acyl phosphate hydrolysis, and thus, the effects of the carboxyamide group and Mg^{2+} would be cumulative, as is observed. In the absence of a defined Spo0F∼P structure, it is difficult to explain the mechanism by which the carboxyamide of residue 56 could promote hydrolysis of the protein acyl phosphate. Nevertheless, the role of Asn 56 in the hydrolysis of Spo0F∼P K56N is reminiscent of the role played by Gln 61 of $p21^{ras}$ in the hydrolysis of GTP. Mutation of Gln 61 reduces the GTPase activity of $p21^{ras}$ by an order of magnitude and leads to ras-proteins with oncogenic properties (*32*). By analogy to this GTPase, the carboxyamide of Asn 56 may position a catalytic water near the protein acyl phosphate or stabilize the transition state to promote Spo0F∼P hydrolysis (Figure 7) (*33, 34*). A similar catalytic role has also been suggested for Asn 41 of horse muscle acylphosphatase, an enzyme structurally unrelated to response regulators but catalyzing a reaction chemically similar to the hydrolysis of phosphorylated response regulators (*35*). However, the possible catalytic similarity between a response regulator and GTPase proteins is noteworthy because both these classes of proteins share a similar protein fold (*36*) and they use the hydrolysis of high energy phosphate moieties to switch from an active to an inactive state (*10*, *32*).

All the Spo0F∼P K56 mutants autodephosphorylate more rapidly than wild-type protein but the molecular basis for this effect may be different for each type of side chain. The side chain of Asn 56 may orient a water molecule and/or stabilize the transition state in the active site of Spo0F K56N. A favorable electrostatic interaction between the alkylamine of Lys 56 and the negatively charged acyl phosphate may retard Spo0F∼P hydrolysis. Consistent with this idea, Spo0F∼P K56M hydrolyzes slightly faster than wild-type Spo0F∼P. In cAMP-dependent protein kinase, comparable electrostatic interactions between three basic side chains (Lys, His, and Arg) and the phosphate of Thr(P) 197 are thought to make this phosphorylated amino acid residue resistant to hydrolysis (*37*). In addition to electrostatic effects, the long side chain of Lys 56 may contribute to the stability of Spo0F∼P since the mutant containing a short side chain at this position Spo0F∼P K56A autodephosphorylates faster than wild-type or K56M proteins. The residue equivalent to position 56 in Spo0F is not a conserved residue and lysine, methionine, alanine, or asparagine occur at this position in many response regulators (*8*). This suggests that response regulators utilize several catalytic strategies to change the protein acyl phosphate hydrolysis rate.

The Role of the Residue Equivalent to 56 in Spo0F in Other Response Regulators. Response regulators share a common structural architecture and it is reasonable to expect the residue at the position equivalent to 56 in Spo0F to have a common function in many members of this protein family. A variety of conditions have been used to measure the autophosphatase activity of various response regulator proteins; nevertheless, a correlation between the type of side chain at this position and the magnitude of the autophosphatase activity is apparent (Table 1). Inefficient autophosphatases ($t_{1/2}$ on the order of hours) tend to have long side chains at the position equivalent to 56 in Spo0F and efficient autophosphatases ($t_{1/2}$ on the order of minutes) frequently contain Asn at this position. Moreover, an observation reported for CheB∼P suggests that the residue equivalent to 56 in Spo0F plays a role in the autophosphatase activity of this chemotaxis response regulator. Mutating the corresponding residue Glu 58 to Lys in CheB∼P diminishes the autophosphatase activity (*38*); thus, the mutant CheB∼P E58K is more "Spo0F∼P-like" in autophosphatase activity. In light of the results presented here, the CheB∼P observation suggests that the carboxylate of Glu 58 in CheB∼P may function like the carboxyamide of Asn 56 in Spo0F∼P K56N, promoting CheB∼P hydrolysis by positioning a catalytic water molecule near the protein acyl phosphate or by stabilizing the transition state. Significantly, carboxylates are similar enough to carboxyamides to allow these functional groups to substitute for each other in the phosphate hydrolysis reaction catalyzed by $p21^{ras}$. For example, the substitution of Glu for the conserved Gln 61 of $p21^{ras}$ does not diminish the intrinsic activity of this GTPase, whereas any other substitution at this position does diminish this activity (*39*). However, it is also possible that the increased length and opposite charge of the Lys relative to the Glu side chain could force a realignment in the CheB∼P active site and disrupt the autophosphatase activity. Further mutations at this site in CheB∼P are required to distinguish between these effects. Nonetheless, it appears that the autophosphatase activity of other phosphorylated response regulators can be affected by the type of residue at the position equivalent to 56 in Spo0F.

The Lys to Asn substitution at position 56 causes Spo0F∼P to autodephosphorylate in minutes. Comparison of response regulators with Asn in this position indicates that Spo0F∼P K56N autodephosphorylates at a rate similar to NarL∼P, but this rate is still more than an order of magnitude slower than the autodephosphorylation rate of CheY∼P (Table 1). To test the idea that either carboxylate or a carboxyamide side chain at position 56 can promote Spo0F∼P hydrolysis, additional mutants at this site are being made. Thus, the nature of the residue in position 56 alone is not sufficient to account for the wide range of autophosphatase rates seen in Table 1. Additional, as yet unknown, structural features must contribute to the autophosphatase rates in some response regulators. Further supporting this idea, NtrC∼P has Val instead of Asn at the position equivalent to 56 in Spo0F and yet exhibits "instability".

Conclusions. With Spo0F∼P, the importance of residue 56 is highlighted by the 23-fold elevation in the autophosphatase activity caused by the Lys to Asn substitution. The enhanced autodephosphorylation of K56 substituted Spo0F∼P contrasts with the usual decrease in catalytic activity associated with mutagenesis. This may imply that the autophosphatase activity of Spo0F∼P has been tempered by evolution. A slow phosphoprotein hydrolysis rate must be an advantageous feature for a response regulator functioning in a signaling cascade, such as the phosphorelay. Hence, it would appear that the major role of a secondary messenger like Spo0F∼P is to authentically transmit the phosphorylation signal and not short-circuit the signal by hydrolysis. Because Lys 56 is located in a loop, any changes in this amino acid residue should not affect the core of the protein, but the close proximity of this residue to the phosphorylation site might allow its side-chain to affect the phosphorylation properties of the active site. NMR structure and dynamic studies with Spo0F indicate the β3 to α3 loop containing Lys 56 is flexible in solution (*40*). Such flexibility may permit the side chain of residue 56 to form contacts with the acyl phosphate that affect Spo0F∼P hydrolysis. It appears that residues in loops adjacent to the active site "tune" the response regulatory autophosphatase activity to suit a particular biological role and also contribute to the specificity observed for histidine kinase/ response regulator pairs (*41*, *42*).

ACKNOWLEDGMENT

We thank Victoria Feher, Tarek Msadek, Yih-Ling Tzeng, and Marta Perego for helpful discussions.

REFERENCES

1. Swanson, R. V., Alex, L. A., and Simon, M. I. (1994) *Trends Biochem. Sci. 19*, 485−490.
2. Roychoudhury, S., Zielinski, N. A., Ninfa, A. J., Allen, N. E., Jungheim, L. N., Nicas, T. I., and Chakrabarty, A. M. (1993) *Proc. Natl. Acad. Sci. U.S.A. 90*, 965−969.
3. Ninfa, A. J., and Magasanik, B. (1986) *Proc. Natl. Acad. Sci. U.S.A. 83*, 5909−5913.
4. Stock, J. B., Surette, M. G., Levit, M., and Park, P. (1995) in *Two-Component Signal Transduction* (Hoch, J. A., and Silhavy, T. J., Eds.) pp 25−51, ASM Press, Washington, DC.
5. Hoch, J. A. (1993) *Annu. Rev. Microbiol. 47*, 441−465.
6. Burbulys, D., Trach, K. A., and Hoch, J. A. (1991) *Cell 64*, 545−552.
7. Perego, M., Hanstein, C., Welsh, K. M., Djavakhishvili, T., Glaser, P., and Hoch, J. A. (1994) *Cell 79*, 1047−1055.
8. Volz, K. (1993) *Biochemistry 32*, 11741−11753.
9. Sanders, D. A., Gillece-Castro, B. L., Stock, A. M., Burlingame, A. L., and Koshland, D. E., Jr. (1989) *J. Biol. Chem. 264*, 21770−21778.
10. Lukat, G. S., Lee, B. H., Mottonen, J. M., Stock, A. M., and Stock, J. B. (1991) *J. Biol. Chem. 266*, 8348−8354.
11. Ganguli, S., Wang, H., Matsumura, P., and Volz, K. (1995) *J. Biol. Chem. 270*, 17386−17393.
12. Madhusudan,, Zapf, J., Whiteley, J. M., Hoch, J. A., Xuong, N. H., and Varughese, K. I. (1996) *Structure 4*, 679−690.
13. Stock, A. M., Martinez-Hackert, E., Rasmussen, B. F., West, A. H., Stock, J. B., Ringe, D., and Petsko, G. A. (1993) *Biochemistry 32*, 13375−13380.
14. Baikalov, I., Schroder, I., Kaczor-Grzeskowiak, M., Grzeskowiak, K., Gunsalus, R. P., and Dickerson, R. E. (1996) *Biochemistry 35*, 11053−11061.
15. Kunkel, T. A., Bebenek, K., and McClary, J. (1991) *Methods Enzymol. 204*, 125−139.
16. Zapf, J. W., Hoch, J. A., and Whiteley, J. M. (1996) *Biochemistry 35*, 2926−2933.
17. Grimsley, J. K., Tjalkens, R. B., Strauch, M. A., Bird, T. H., Spiegelman, G. B., Hostomsky, Z., Whiteley, J. M., and Hoch, J. A. (1994) *J. Biol. Chem. 269*, 16977−16982.
18. Frieden, C. (1994) *Methods Enzymol. 240*, 311−322.
19. Madhusudan,, Zapf, J., Hoch, J. A., Whiteley, J. M., Xuong, N. H., and Varughese, K. I. (1997) *Biochemistry 36*, 12739−12745.
20. Ward, L. D. (1985) *Methods Enzymol. 117*, 400−414.
21. Bradford, M. M. (1976) *Anal. Biochem. 72*, 248−254.
22. Feher, V. A., Zapf, J. W., Hoch, J. A., Dahlquist, F. W., Whiteley, J. M., and Cavanagh, J. (1995) *Protein Sci. 4*, 1801−1814.
23. Lukat, G. S., Stock, A. M., and Stock, J. B. (1990) *Biochemistry 29*, 5436−5442.
24. Stock, J. B., Ninfa, A. J., and Stock, A. M. (1989) *Microbiol. Rev. 53*, 450−490.
25. Parkinson, J. S., and Kofoid, E. C. (1992) *Annu. Rev. Genet. 26*, 71−112.
26. Perego, M., and Hoch, J. A. (1996) *Trends Genet. 12*, 97−101.
27. Grossman, A. D. (1995) *Annu. Rev. Genet. 29*, 477−508.
28. Simms, S. A., Keane, M. G., and Stock, J. (1985) *J. Biol. Chem. 260*, 10161−10168.
29. Igo, M. M., Ninfa, A. J., Stock, J. B., and Silhavy, T. J. (1989) *Genes Dev. 3*, 1725−1734.
30. Tzeng, Y., and Hoch, J. A. (1997) *J. Mol. Biol. 272*, 200−212.
31. Knowles, J. R. (1980) *Annu. Rev. Biochem. 49*, 877−919.
32. Kjeldgaard, M., Nyborg, J., and Clark, B. F. C. (1996) *FASEB J. 10*, 1347−1368.
33. Scheffzek, K., Ahmadian, M. R., Kabsch, W., Wiesmuller, L., Lautwein, A., Schmitz, F., and Wittinghofer, A. (1997) *Science 277*, 333−338.
34. Maegley, K. A., Admiraal, S. J., and Herschlag, D. (1996) *Proc. Natl. Acad. Sci. U.S.A. 93*, 8160−8166.
35. Taddei, N., Stefani, M., Magherini, F., Chiti, F., Modesti, A., Raugei, G., and Ramponi, G. (1996) *Biochemistry 35*, 7077−7083.
36. Artymiuk, P. J., Rice, D. W., Mitchell, E. M., and Willett, P. (1990) *Protein Eng. 4*, 39−43.
37. Taylor, S. S., Knighton, D. R., Zheng, J., Ten Eyck, L. F., and Sowadski, J. M. (1992) *Annu. Rev. Cell Biol. 8*, 429−462.
38. Stewart, R. C. (1993) *J. Biol. Chem. 268*, 1921−1930.
39. Frech, M., Darden, T. A., Pedersen, L. G., Foley, C. K., Charifson, P. S., Anderson, M. W., and Wittinghofer, A. (1994) *Biochemistry 33*, 3237−3244.
40. Feher, V. A., Zapf, J. W., Hoch, J. A., Whiteley, J. M., McIntosh, L. P., Rance, M., Skelton, N. J., Dahlquist, F. W., and Cavanagh, J. (1997) *Biochemistry 36*, 10015−10025.
41. Ninfa, A. J., Ninfa, E. G., Lupas, A. N., Stock, A., Magasanik, B., and Stock, J. (1988) *Proc. Natl. Acad. Sci. U.S.A. 85*, 5492−5496.
42. Fisher, S. L., Jiang, W., Wanner, B. L., and Walsh, C. T. (1995) *J. Biol. Chem. 270*, 23143−23149.
43. Keener, J., and Kustu, S. (1988) *Proc. Natl. Acad. Sci. U.S.A. 85*, 4976−4980.
44. Cavicchioli, R., Schroder, I., Constanti, M., and Gunsalus, R. P. (1995) *J. Bacteriol. 177*, 2416−2424.
45. Fisher, S. L., Kim, S. K., Wanner, B. L., and Walsh, C. T. (1996) *Biochemistry 35*, 4732−4740.
46. Wright, G. D., Holman, T. R., and Walsh, C. T. (1993) *Biochemistry 32*, 5057−5063.
47. McCleary, W. R. (1996) *Mol. Microbiol. 20*, 1155−1163.

BI9729615